

840 mW continuous-wave Fe:ZnSe laser operating at 4140 nm

Jonathan W. Evans,* Patrick A. Berry, and Kenneth L. Schepler

Air Force Research Laboratory, Sensors Directorate, 2241 Avionics Circle, Wright-Patterson AFB, Ohio 45433, USA

*Corresponding author: jonathan.evans@wpafb.af.mil

Received September 17, 2012; revised October 22, 2012; accepted October 22, 2012;
posted October 23, 2012 (Doc. ID 176326); published November 30, 2012

We report the demonstration of high-power (840 mW) continuous-wave laser oscillation from Fe²⁺ ions in zinc selenide. The output spectrum of the Fe:ZnSe laser had a line-center near 4140 nm with a linewidth of 80 nm. The beam quality was measured to be $M^2 \leq 1.2$ with a maximum slope efficiency of 47%. Small shifts observed in output wavelength with increased output power were attributed to thermal effects. No thermal roll-off of slope efficiency was observed at the maximum of output power. © 2012 Optical Society of America

OCIS codes: 140.3580, 140.3070.

Solid-state infrared lasers are of interest for many applications, including remote sensing, laser radar, infrared laser spectroscopy, and for other military, scientific, and commercial purposes. Yet few direct laser sources operate in the 3–5 μm atmospheric transmission window. High-power lasing has been demonstrated in the 2–3 μm region from Cr²⁺ ions doped into various II–VI crystal hosts [1], most notably ZnSe [2] and ZnS [3]. These lasers are capable of tens of watts of CW output power [4], are broadly tunable [2,3], and can achieve high peak powers via Q-switched or mode-locked operation [5]. Fe²⁺ ions and Cr²⁺ ions have complementary electronic configurations and thus exhibit similar spectroscopic properties. However, Fe²⁺ ions experience a smaller crystal field splitting in II–VI hosts than do Cr²⁺ ions. Consequently, the optical emission of Fe:ZnSe is greatest from 3.5 to 5 μm , making this material a promising candidate for a high-power tunable laser in this region.

The room temperature upper-state lifetime of Fe²⁺ in ZnSe is 370 ns [6], making it difficult to maintain population inversion. The radiative lifetime of Fe²⁺ in ZnSe is a maximum of 105 μs near 120 K [7]. By operating at 77 K, Voronov *et al.* achieved 200 mW of CW optical output power from an Fe:ZnSe laser operating from 4040 to 4080 nm. They achieved a slope efficiency of 56% using single crystal Fe:ZnSe [8,9]. In this Letter, we report a four-fold increase in the CW output power from an Fe:ZnSe laser with high beam quality.

We employed a polycrystalline ZnSe sample diffusion-doped with Fe²⁺ ions to a concentration of approximately $9 \times 10^{18} \text{ cm}^{-3}$ as reported by the vendor [10]. Fe:ZnSe exhibits a broadband absorption feature with a local maximum at $\lambda \approx 3100 \text{ nm}$ at both room temperature and cryogenic temperatures (see Fig. 1 [11]). This absorption band can be pumped using the $\lambda = 2940 \text{ nm}$ Er²⁺:YAG laser transition. We pumped the Fe:ZnSe laser cavity from each end with a Sheamann Laser MIR-PAC microchip laser. The maximum CW output power of each laser was 1.5 W; thus, a maximum of 3 W of total pump power was available at 2940 nm.

To minimize the mode size in the crystal and given the constraints of the dewar, we constructed a nearly concentric spherical laser cavity with 50 mm radius of curvature end mirrors M1 and M2, as shown in Fig. 2. M2 also functioned as an outcoupler with $R \approx 70\%$ from

3000 to 5000 nm. The pump beams each exhibited $M^2 \leq 2$ and each beam was collimated using lenses L1 and L2 as shown. Each collimated pump beam was focused through a cavity mirror and into the center of the Fe:ZnSe sample. We used two $f = 150 \text{ mm}$ lenses L3 and L4 to obtain $1/e^2$ beam waist diameters of 220 μm . The Fe:ZnSe sample measured 2 mm \times 6 mm \times 8 mm and was wrapped in indium foil and clamped to a copper mount cooled to $\sim 77 \text{ K}$ by liquid nitrogen. The two smallest facets of the crystal and windows W1 and W2 were broadband anti-reflection (AR) coated from 2900 to 5000 nm. The sample compartment was evacuated to $\sim 1 \text{ mTorr}$. The output beam was separated from the pump beam using a dichroic mirror M3, which exhibited $R > 97\%$ from 3000 to 5000 nm.

Together, L1, L3, and M1 transmitted only 81% of the power from P1. The threshold of lasing was 150 mW and the ratio of transmitted power to output power showed 37% slope efficiency (see Fig. 3). The combination of L2, L4, M3, and M2 transmitted only 64% of the power from P2. Thus, with both pump beams operating at full power, only 2.17 W of pump power was coupled into the cavity. The slope efficiency of the laser with respect to P2 was measured to be 47% with P1 operating at full power. With

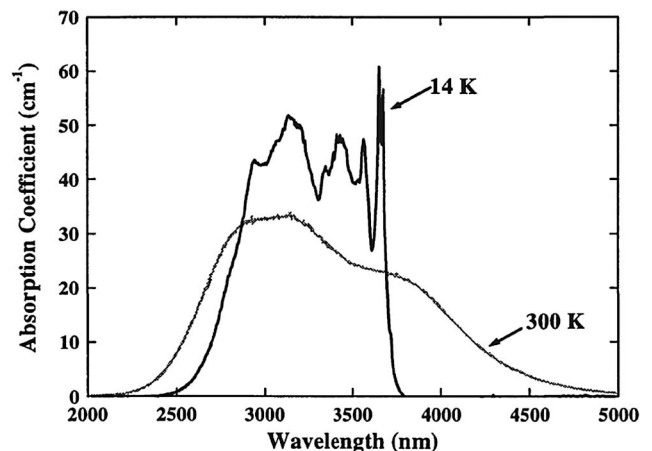


Fig. 1. Absorption coefficient of Fe²⁺ in ZnSe at 77 and 300 K (modified from [11] with permission from the Optical Society of America).

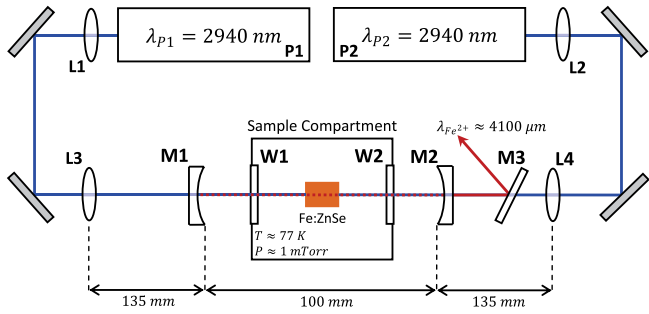


Fig. 2. (Color online) Schematic view of the Fe:ZnSe laser design. All optics are made of CaF₂ and AR-coated at 2940 nm unless otherwise noted.

both pump lasers at full power, the maximum output of the laser was 847 ± 12 mW.

The values of input power shown in Fig. 3 are direct measurements of the power incident on W1 or W2. From direct measurement of the transmission and reflection of M3 at the pump wavelength, we were able to determine that <1 mW of the power measured in reflection from M3 can be attributed to content at 2940 nm. We note that for all data points of Fig. 3 this correction is less than the measured uncertainty of the output power and has thus been neglected.

The lack of thermal roll-off in Fig. 3 suggests that thermal lensing in the crystal is weak. We used the method of [12] to calculate a maximum thermal lens power of 16 m^{-1} at full power. We constructed a model of the laser cavity including all the beam parameters reported in this Letter. With this model, we calculated the $1/e^2$ beam waist diameter to be $265 \mu\text{m}$ at the center of the crystal in the absence of thermal lensing and to be $<300 \mu\text{m}$ when thermal lensing effects were considered.

To measure the beam quality of the Fe:ZnSe laser, the output beam was focused using a 100 mm lens. The $1/e^2$ radius $w(z)$ of the focused beam was measured at evenly spaced locations along the optic axis using a Photon Inc. Nanoscan scanning slit beam profiler. The beam quality M^2 and the beam waist radius w_0 were determined as parameters of a least-squares fit of the beam width data to

$$w(z) = w_0 \cdot \sqrt{1 + M^2 \left(\frac{z}{z_R} \right)^2},$$

where z_R is the Rayleigh range of the beam, w_0 is the beam waist radius, and the zero of z is defined at the

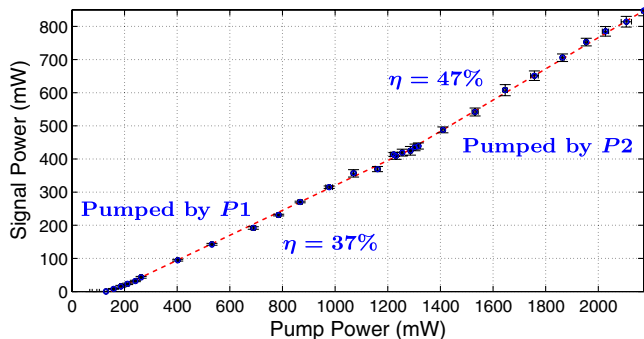


Fig. 3. (Color online) Slope efficiency plot of the Fe:ZnSe laser. Error bars correspond to $\pm\sigma/2$.

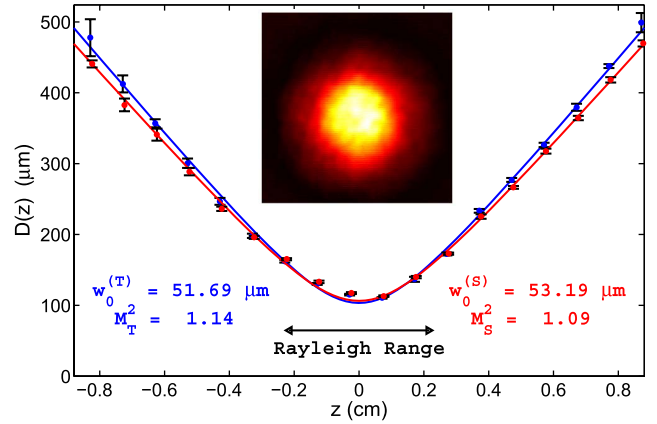


Fig. 4. (Color online) Beam profile of the Fe:ZnSe laser operating at full power (T \rightarrow Transverse and S \rightarrow Sagittal). The inset is a picture of the beam as recorded by an Electrophysics PV320 camera.

beam waist. Figure 4 shows the profile of the output beam. When pumping with P1 at full power and P2 off we measured $M_T^2 = 1.14$ and $M_S^2 = 1.09$. When pumping with both P1 and P2 at full power we measured $M_T^2 = 1.08$ and $M_S^2 = 1.13$.

The laser output at full power was spectrally resolved using an Acton SpectraPro-750 monochromator. The instrument utilized a 300 groove/mm grating blazed at $3 \mu\text{m}$. The real-time (50 Hz) spectrum of the laser was recorded using a CalSensors PbSe linear detector array at the output port of the monochromator. The observed spectrum indicated that the laser operated on many longitudinal modes of the cavity simultaneously. The relative amplitude of each mode fluctuated rapidly, consistent with mode-hopping.

The output spectrum of the laser was also recorded using a liquid nitrogen cooled InSb detector with the slit widths set to $10 \mu\text{m}$ to give the instrument a spectral resolution of $<0.5 \text{ nm}$. Datasets of 15 samples each were collected in 1 nm intervals with an integration time of 300 ms. The output spectrum of Fig. 5 shows the average value of each interval. The spectral centroid of the output trended

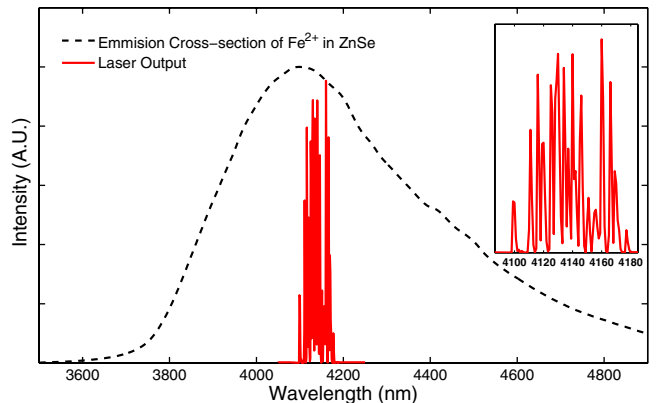


Fig. 5. (Color online) Emission spectrum of the Fe:ZnSe laser operating at full power. The dotted line is the relative emission cross section of Fe²⁺ in ZnSe at 77 K as calculated from a system-compensated emission spectrum and the Füchtbauer-Ladensburg equation. The inset shows the lasing region in greater detail.

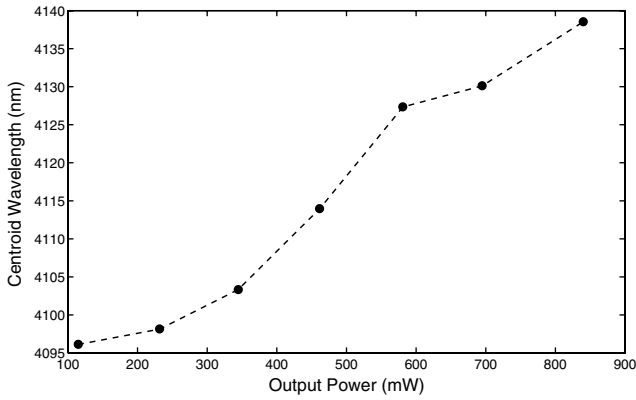


Fig. 6. Spectral centroid position as a function of increasing output power.

toward longer wavelengths with increasing output power as shown in Fig. 6. The time-averaged spectral width of the laser output was 60–80 nm for all values of output power.

We attribute this shift in the spectral content of the laser output to an increase in temperature at the focus of the pump laser. This localized heating of the crystal changes the distribution of population among the energy levels of the lasing ion. This change preferentially increases the probability of reabsorption of the shorter-wavelength photons emitted from the broad energy levels of the Fe^{2+} ion and shifts the peak gain of the material to longer wavelengths.

We support our claim that the redshift is due to thermal effects by comparing the output spectrum of the free-running Fe:ZnSe laser to the output spectrum of the laser recorded when P1 was chopped at 200 Hz with a 50% duty cycle. With P2 off, we observed that the time-averaged spectral centroid of the laser output decreased by ~12 nm when P1 was chopped. This observation is consistent with Fig. 6, and suggests that the redshifts follow changes in average pump power, not peak pump power. Thus, we conclude that the observed redshifts are due to thermal effects within the crystal and not to intensity-dependent dynamics of the Fe^{2+} ions.

We observed that using a different ZnSe sample with a lower quoted concentration of Fe^{2+} ions resulted in a shift of the spectral centroid of the laser output toward the blue by tens of nanometers. This effect is due to a decrease in reabsorption of emitted photons at shorter wavelengths. It is not clear whether the preferential

decrease in reabsorption is a direct consequence of reducing the concentration or an indirect consequence of thermal effects due to decreased absorption of pump power.

In conclusion, we have achieved 840 mW of CW output power at 4140 nm with $M^2 < 1.2$ beam quality from a doubly pumped Fe:ZnSe laser. Neglecting coupling losses, the optical efficiency of the laser was 39% at full power. The output power of the laser was limited by pump power with no indication of thermal roll-off.

We acknowledge and thank the Air Force Office of Scientific Research (AFOSR) and the Sensors Directorate for funding this research.

References

1. L. DeLoach, R. Page, G. Wilke, S. Payne, and W. Krupke, *IEEE J. Quantum Electron.* **32**, 885 (1996).
2. J. B. McKay, W. B. Roh, and K. L. Schepler, in *Conference on Lasers and Electro-Optics*, (Optical Society of America, 2002), Vol. **73**, pp. 119–120.
3. I. T. Sorokina, E. Sorokin, S. Mirov, V. Fedorov, V. Badikov, V. Panyutin, and K. I. Schaffers, *Opt. Lett.* **27**, 1040 (2002).
4. I. S. Moskalev, V. V. Fedorov, S. B. Mirov, P. A. Berry, and K. L. Schepler, in *Advanced Solid-State Photonics* (Optical Society of America, 2008), p. WB30.
5. C. R. Pollock, N. A. Brilliant, D. Gwin, T. J. Carrig, W. J. Alford, J. B. Heroux, W. I. Wang, I. Vurgaftman, and J. R. Meyer, in *Advanced Solid-State Photonics* (Optical Society of America, 2005), p. 252.
6. V. Fedorov, S. Mirov, A. Gallian, D. Badikov, M. Frolov, Y. Korostelin, V. Kozlovsky, A. Landman, Y. Podmar'kov, V. Akimov, and A. Voronov, *IEEE J. Quantum Electron.* **42**, 907 (2006).
7. J. J. Adams, C. Bibeau, R. H. Page, D. M. Krol, L. H. Furu, and S. A. Payne, *Opt. Lett.* **24**, 1720 (1999).
8. A. A. Voronov, V. I. Kozlovskii, Y. V. Korostelin, A. I. Landman, Y. P. Podmar'kov, Y. K. Skasyrskii, and M. P. Frolov, *Quantum Electron.* **38**, 1113 (2008).
9. V. I. Kozlovsky, V. A. Akimov, M. P. Frolov, Y. V. Korostelin, A. I. Landman, V. P. Martovitsky, V. V. Mislavskii, Y. P. Podmar'kov, Y. K. Skasyrsky, and A. A. Voronov, *Physica Status Solidi (b)* **247**, 1553 (2010).
10. IPG Photonics, personal communication (2010).
11. J. J. Adams, C. Bibeau, R. H. Page, and S. A. Payne, in *Advanced Solid State Lasers* (Optical Society of America, 1999), p. WD3.
12. K. L. Schepler, R. D. Peterson, P. A. Berry, and J. B. McKay, *IEEE J. Quantum Electron.* **11**, 713 (2005).